

---

# VISTAQA: Benchmarking Joint Visual Question Answering and Pixel-Level Evidence

---

Mozhgan Nasr Azadani<sup>1,2</sup>, Yimu Wang<sup>1</sup>, Yongpeng Zhu<sup>1,\*</sup>, Lihong Chen<sup>1,\*</sup>, Milan Ganai<sup>2</sup>, Sean Sedwards<sup>1</sup>, Marco Pavone<sup>2,3,†</sup>, Krzysztof Czarnecki<sup>1,†</sup>  
<sup>1</sup> University of Waterloo, <sup>2</sup> Stanford University, <sup>3</sup> NVIDIA

Project Page: <https://vistaqa.github.io>

## Abstract

Establishing a clear link between model predictions and the visual evidence that supports them is critical for transparency and reliability in multimodal reasoning, yet current multimodal large language model (MLLM) evaluations do not explicitly enforce this alignment. Existing benchmarks assess either textual answer correctness or pixel-level localization in isolation, leaving the coupling of reasoning and grounding an open challenge. We introduce VISTAQA, a comprehensive benchmark for joint evaluation of free-form answer correctness and pixel-level evidence grounding in visual question answering. VISTAQA comprises 1,157 expert-curated samples spanning six task types and six visual domains, ranging from direct perception to compositional and relational reasoning. VISTAQA requires models to not only answer correctly, but to also provide precise segmentation masks that support their answers. It also includes hallucination-aware examples where no valid visual evidence exists. To support this enhanced evaluation, we introduce GROVE, a unified evaluation metric that enforces joint correctness by combining textual accuracy and grounding quality via a per-sample geometric mean, ensuring neither dimension can compensate for deficiencies in the other. Comprehensive experiments across grounding-aware models and hybrid pipelines with general-purpose MLLMs reveal that even the strongest systems achieve limited performance under GROVE, highlighting a substantial gap between answer accuracy and visual evidence alignment.

## 1 Introduction

Multimodal large language models (MLLMs) have demonstrated remarkable progress across a wide range of multimodal tasks, including visual question answering (VQA), image captioning, and compositional reasoning [5, 6, 36, 37, 42]. Despite these advances, standard evaluation protocols [21, 28, 46] continue to assess performance primarily through textual correctness. A model is rewarded for producing the right answer, even when that answer is not supported by the appropriate visual evidence. Conversely, a model may produce plausible but incorrect answers driven by language priors, despite contradictory visual cues (e.g., answering “two” legs for an animal that visibly has three [34]) [8, 13, 19]. This creates a fundamental limitation: textual correctness alone cannot determine whether a reply is truly grounded in the image, an essential requirement for model interpretability and hallucination mitigation. For reliable deployment in real-world settings, models must be evaluated on not only *what they say*, but also *what visual evidence* supports their statements.

---

\* Equal contribution. † Equal advising.

Correspondence to: [mnasraza@uwaterloo.ca](mailto:mnasraza@uwaterloo.ca)

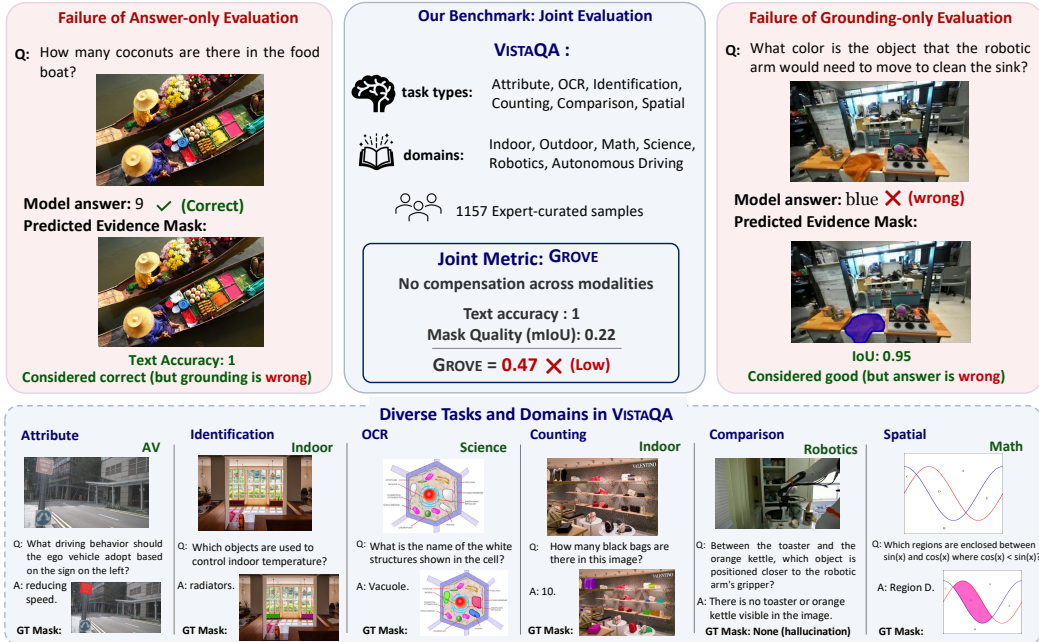


Figure 1: VISTAQA jointly evaluates answer correctness and pixel-level evidence across six tasks and six domains, requiring both to be correct and preventing compensation between modalities.

Recent efforts toward grounding have emerged from two complementary but largely disconnected directions. On one hand, reasoning segmentation models [17, 29, 38, 40, 41] demonstrate strong pixel-level localization capabilities, but they are not optimized for generating rich, free-form textual answers and have been reported to achieve limited success on general VQA benchmarks [48]. On the other hand, state-of-the-art MLLMs [11, 26] achieve high accuracy on complex multimodal reasoning tasks, but typically do not produce explicit visual evidence to substantiate their predictions. While more recent visual grounding approaches [27, 35, 44, 45] begin to bridge this gap, their textual and visual capabilities are still largely evaluated in isolation: models are scored on answer accuracy and segmentation quality as separate metrics, usually on different datasets (*e.g.*, VQA benchmarks for text and segmentation datasets for masks). Consequently, existing evaluation protocols do not enforce alignment between answers and their supporting visual evidence, leaving the coupling of reasoning and grounding an open challenge.

Existing benchmarks reflect and reinforce this divide. VQA benchmarks [9, 12, 22, 47] evaluate compositional reasoning through textual answers, but provide no mechanism to verify whether those answers are grounded in the correct image regions. Conversely, referring expression and reasoning segmentation benchmarks [17, 30, 43] emphasize localization, but treat segmentation as the prediction target rather than as evidence supporting a textual answer. More recent efforts attempt to combine answering and grounding signals; however, grounding is typically treated as a referring or auxiliary output rather than explicit evidence [4, 39], and evaluation protocols assess answer correctness and localization quality independently, without enforcing consistency between them [35, 45]. In addition, these benchmarks are often limited to narrow domains or task settings and rarely account for hallucination, where models must recognize the absence of valid visual evidence. As a result, there remains no benchmark that systematically requires models to produce correct free-form answers that are explicitly supported by pixel-level visual evidence across diverse tasks and domains.

To address this gap, we introduce VISTAQA, a benchmark for the joint evaluation of free-form answer correctness and pixel-level evidence grounding in VQA. Each sample in VISTAQA consists of a question, a reference answer, and a segmentation mask that specifies the visual evidence required to support that answer. Current state-of-the-art MLLMs are insufficiently reliable to autonomously generate complex image-question-mask triplets end-to-end, so constructing a benchmark that jointly evaluates answer correctness and pixel-level evidence grounding requires rigorous human control at every stage of the pipeline. VISTAQA thus comprises 1,157 carefully curated samples spanning six task types, including *identification*, *attribute*, *OCR*, *spatial*, *counting*, and *comparison* and six visual domains, including *indoor*, *outdoor*, *autonomous driving*, *robotics*, *science*, and *mathematics*.

These tasks cover the spectrum from direct perceptual recognition to compositional and relational reasoning in diverse real-world settings. These tasks and domains are illustrated in Figure 1. Notably, VISTAQA includes hallucination-aware samples, where questions are unanswerable or refer to absent entities, requiring models to correctly identify the absence of valid visual evidence.

We formulate evaluation as a *joint correctness* problem: a prediction is considered fully correct only when both the textual answer and the corresponding evidence mask are correct. To support this setting, we introduce GROVE (**GRO**unded **eV**idence **E**valuation), a unified metric that jointly measures answer correctness and grounding fidelity by computing a per-sample geometric mean of smoothed text and mask scores, ensuring that both dimensions are satisfied simultaneously. GROVE is designed around two key desiderata: (1) *joint sensitivity*, penalizing failures in either modality, and (2) *graceful degradation*, preserving signal under partial correctness, while remaining applicable across diverse model classes and evaluation settings.

Our main contributions are as follows:

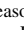
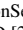

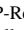
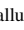

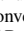
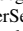



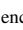




- We introduce VISTAQA, a comprehensive benchmark for the joint evaluation of free-form answers and pixel-level supporting evidence across six tasks and six domains, with explicit hallucination-aware scenarios.
- We propose GROVE, a unified evaluation metric that jointly measures answer correctness and grounding fidelity by computing a per-sample geometric mean of smoothed text and mask scores, ensuring that both dimensions are satisfied simultaneously.
- We conduct comprehensive experiments across state-of-the-art baselines on VISTAQA, demonstrating that even the strongest current models struggle to align answers with correct visual evidence.

## 2 Related work

Early benchmarks for vision-language understanding focused on isolated capabilities, limiting their ability to evaluate grounded reasoning. VQA benchmarks have evolved from basic visual recognition [1, 12] toward compositional and multi-hop reasoning [9, 47], with subsequent efforts expanding coverage to specialized domains such as autonomous driving [24, 32] and mathematics [22], as well as to more challenging tasks such as hallucination mitigation [13, 49]. Despite this breadth, VQA benchmarks evaluate correctness at the textual level and do not require models to provide explicit visual evidence supporting their answers. A complementary line of work focuses on grounding through segmentation. Referring expression datasets [23, 29, 40, 43] require models to localize objects described by natural language. More recent benchmarks extend this to reasoning-centric settings [17, 18, 30], introducing increasingly complex queries, counterfactual scenarios, and ambiguity. However, these benchmarks continue to treat segmentation masks as the primary prediction target. Despite their individual advances, the above benchmarks evaluate either *what* models answer or *where* they localize, but do not explicitly require answers to be grounded in visual evidence.

More recent benchmarks attempt to bridge the gap between VQA and grounded localization, yet critical limitations persist across three dimensions: grounding role, reasoning depth, and evaluation scope. Early efforts, such as VizWiz-Grounding [4] and V\*Bench [39], pair questions with visual localization, but treat grounding as a referring mechanism, identifying *where* an answer object is located, rather than as evidence for *why* an answer is correct. The works most closely related to ours are VRT-Bench [45] and TreeBench [35], which move toward evidence-based grounding. VRT-Bench associates reasoning steps with segmentation masks as supporting evidence, while TreeBench introduces structured reasoning with traceable bounding box signals. However, as summarized in Table 1, both still evaluate text and grounding independently, rather than enforcing consistency between them. They remain confined to a single domain and do not explicitly assess hallucination robustness, leaving a critical gap in comprehensive grounded evaluation. VISTAQA is designed to bridge this gap by introducing a unified evaluation metric that jointly assesses answer correctness and pixel-level grounding fidelity. The proposed metric enables a rigorous evaluation of whether model predictions are both factually accurate and visually supported. Spanning six tasks and six domains, VISTAQA covers a spectrum from basic perception to high-level reasoning across diverse real-world settings, while explicitly accounting for model hallucination.

Table 1: Comparison of recent benchmarks for grounded VQA and segmentation. MC: Multiple Choice; Acc.: Text Accuracy.

Name	Test Size	VQA / Q type	Grounding	Halluc.	#Tasks	#Domains	Annot.	Metric
ReasonSeg [17]	779	×	mask (reasoning)	×	1	1	 	gIoU
GranD [29]	5000	×	mask (referring)	×	1	1		mIoU
FP-RefCOCO [40]	1500	×	mask (referring)	✓	1	1		cloU
HalluSegBench [18]	399	×	mask (reasoning)	✓	1	1	 	CMS, mIoU
ConverSeg [30]	1687	×	mask (reasoning)	✓	4	1	 	gIoU
V <sup>*</sup> Bench [39]	191	✓ / MC	bbox (referring)	×	2	1		Acc.
VizWiz-VQA-Gr [4]	2373	✓ / free-form	bbox (referring)	×	1	1		mIoU
TreeBench [35]	405	✓ / MC	bbox (evidence)	×	10	1	 	Acc., mIoU
VRT-Bench [45]	304	✓ / free-form	mask (evidence)	×	4	1	 	Acc., mIoU
<b>VISTAQA (ours)</b>	<b>1157</b>	<b>✓ / free-form</b>	<b>mask (evidence)</b>	<b>✓</b>	<b>6</b>	<b>6</b>	 	<b>Joint (GROVE)</b>

### 3 VISTAQA Benchmark

We introduce VISTAQA, a comprehensive benchmark for the joint evaluation of answer correctness and pixel-level evidence grounding in VQA. Unlike prior benchmarks that assess text and grounding independently, VISTAQA requires models to produce a free-form answer alongside a segmentation mask that serves as explicit visual evidence supporting that answer. A prediction is considered correct only when both the answer and the corresponding mask are valid, enabling rigorous assessment of whether model outputs are both accurate and visually grounded.

#### 3.1 Tasks and Domains

VISTAQA comprises 1,157 curated samples covering six task types and six visual domains, including 314 hallucination samples ( $\approx 27\%$ ) specifically designed to probe robustness against visually misleading or unanswerable queries. Figure 1 illustrates representative examples from all task types. Detailed definitions are provided in Appendix A.1.

**Tasks.** VISTAQA’s six task types span a spectrum from direct visual perception to higher-order reasoning, reflecting the diverse cognitive demands of grounded VQA. Perception-oriented tasks (*identification*, *attribute*, and *OCR*) evaluate first-order visual understanding, where correct answers depend on accurately localizing a target region and directly interpreting its properties. Reasoning-oriented tasks (*spatial*, *counting*, and *comparison*) require higher-order inference over multiple regions, involving relational, enumerative, or comparative reasoning beyond direct recognition.

**Domains.** VISTAQA’s six visual domains are designed to capture the diversity of real-world settings in which grounded visual reasoning is required. Together, they span a broad spectrum of visual characteristics and reasoning demands, from natural scenes to structured diagrams, and from passive perception to embodied interaction, enabling comprehensive evaluation of model robustness across diverse scenarios: (1) *indoor* and (2) *outdoor* environments represent everyday scenes with varying object density, lighting, and contextual complexity, testing robust grounded understanding in general settings; (3) *autonomous driving* introduces safety-critical scenarios with dynamic agents and structured road semantics; (4) *robotics* focuses on embodied interaction and manipulation-centric reasoning, where tasks depend on accurately localizing objects and reasoning about their spatial configuration and affordances; (5) *science* includes domain-specific visual content such as diagrams, charts, and biological or physical schematics, requiring grounding over structured representations that combine perceptual and domain knowledge; and (6) *math* emphasizes geometric interpretation and diagram-based reasoning.

#### 3.2 Benchmark Construction

Constructing a benchmark that jointly evaluates answer correctness and pixel-level evidence grounding requires rigorous control at every stage of the pipeline. A key challenge is that current state-of-the-art MLLMs are insufficiently reliable to autonomously generate complex image-question-mask triplets end-to-end. In particular, MLLMs can introduce systematic errors in QA generation for certain tasks (see Appendix A.6), while reasoning segmentation models often fail to produce accurate masks when prompted with complex or domain-specific queries, rendering fully automated construction unreliable. Accordingly, VISTAQA is constructed using a systematic multi-stage pipeline that combines domain-appropriate image sourcing, hybrid mask generation, LLM-assisted QA generation,

and multi-round human verification, ensuring that each sample satisfies strict standards of visual quality, answer correctness, and grounding fidelity.

**Image Collection and Generation.** We sample approximately 300 images per domain from five existing datasets and generate 200 synthetic images for the mathematics domain, with deliberate emphasis on visual complexity and reasoning challenge. For *indoor* and *outdoor* scenes, images are sampled from SA-1B [15], which offers high-resolution, real-world scenes with a large number of small and varied objects, making it particularly suitable for evaluating visually grounded reasoning across everyday environments. *Autonomous driving* images are sampled from NuScenes [2], capturing complex multi-agent scenarios with safety-critical objects and structured road semantics. *Robotics* images are sampled from the DROID dataset [14], focusing on manipulation and interaction scenes that demand fine-grained spatial and object-level understanding. *Science* images are sampled from ScienceQA [31], covering domain-specific diagrams, charts, and illustrations that require grounding in structured visual representations. For *mathematics*, images are generated using custom scripts, enabling precise control over geometric configurations, symbolic layouts, and ground-truth answers.

**Mask Generation and Extraction.** Segmentation masks are constructed using domain-specific strategies tailored to the characteristics of each data source. For *indoor* and *outdoor* domains, masks are directly extracted from existing SA-1B annotations, providing high-quality pixel-level segmentations. For *mathematics*, masks are generated programmatically alongside the images, ensuring exact correspondence between visual content and evidence regions. For *autonomous driving*, *robotics*, and *science* domains, masks are obtained through a combination of automated segmentation using SAM3 [3] and human annotation. In practice, SAM3 often fails to reliably isolate specific instances from text prompts and struggles with sub-structure recognition in specialized domains (*e.g.*, distinguishing fine-grained biological components such as organelles). To address these limitations, annotators manually draw or refine masks to accurately delineate the intended evidence regions.

**Question-Answer Generation.** For each image, we use two MLLMs, GPT-5.2 [25] and Gemini 3 Pro [10], to independently generate five candidate QA pairs each, conditioned on the image, task type, and a structured prompt template crafted to ensure grounding-aware question complexity and precise visual-semantic correspondence (see Appendix A.7). To evaluate models tendency to hallucinate, we also include an adversarial objective: models must generate three negative candidates involving non-existent entities, invalid spatial relations, or multi-hop reasoning anchored in absent attributes. Human annotators then select the most semantically precise candidate from the resulting pool of ten/six, or manually compose or refine QA for task types when automated generation consistently fails, most notably for reasoning-intensive tasks such as *counting*.

**Quality Control** is applied at three stages of the pipeline. Following mask generation, annotators verify image and mask quality, ensuring that each mask accurately captures the intended evidence region. Following QA generation, annotators evaluate each candidate *w.r.t.* the intended reasoning skill, precision of visual grounding, and clarity of answerability, selecting the most semantically precise candidate or performing manual refinement when necessary. A final cross-validation round by independent annotators ensures the coherence and consistency of the complete question-answer-mask triplet. The final benchmark comprises 1,157 samples after rigorous quality filtering.

### 3.3 Statistics

The distribution of VISTAQA’s task types and domains is illustrated in Figure 2. Task types are balanced between perception and reasoning categories, with individual tasks ranging from 173 (OCR, 15.0%) to 214 (Identification, 18.5%) samples. This balance is deliberate: unlike benchmarks that emphasize higher-order reasoning, VISTAQA evaluates grounding fidelity across the full spectrum of visual cognition, reflecting the requirement that evidence grounding must remain reliable regardless of task complexity. Figure 2b shows that approximately 27.1% of samples (314) consist of hallucination cases where no valid grounding exists, explicitly probing model robustness to misleading or unanswerable queries. The remaining 72.9% (843) correspond to grounded scenarios with at least one annotated evidence mask. Domain coverage is similarly balanced across all six visual settings, ensuring that evaluation is not confounded by domain bias.

Mask multiplicity follows a long-tailed distribution (Figure 2c), where the 314 zero-instance samples correspond to hallucination cases in which the queried entity is absent by design. Among the 843 grounded samples, 70.6% contain a single mask instance, reflecting the prevalence of precise,

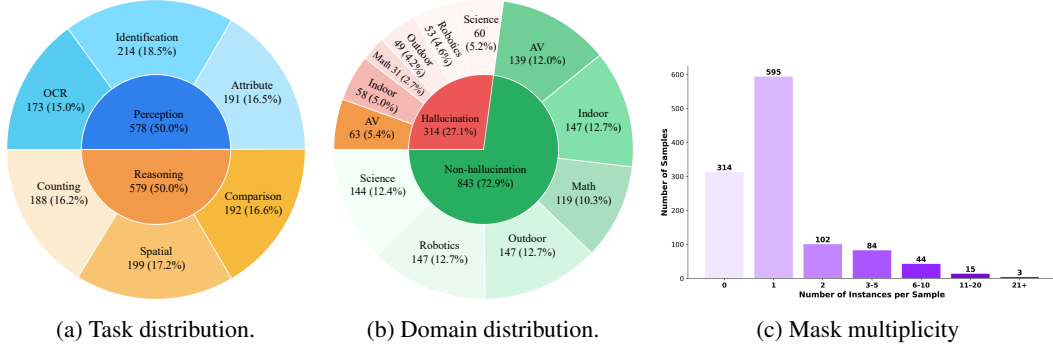


Figure 2: VISTAQA dataset statistics. The benchmark is balanced across task types (a) and across domains for hallucination and non-hallucination samples (b). Mask multiplicity follows a long-tailed distribution driven primarily by *counting* tasks, where the zero-instance samples correspond to hallucination cases (c).

localized evidence grounding, while 29.4% contain two or more instances, with a long tail extending to a maximum of 57 masks per sample. Overall, single- and dual-instance samples account for 82.7% of grounded samples, indicating a balance between grounding precision and compositional complexity. Multi-instance scenarios, driven primarily by *counting* tasks (mean of 3.89 masks per sample), further stress-test instance-level grounding in dense scenes.

### 3.4 Evaluation Metric

We introduce GROVE (**GR**ounded **eV**idence **E**valuation), a unified metric designed around two key desiderata: (1) *joint sensitivity*, where neither text nor mask correctness alone is sufficient for a high score, and (2) *graceful degradation*, where partial correctness along one axis contributes a meaningful signal rather than collapsing to zero.

**Answer Score** ( $S_a \in \{0, 1\}$ ) is a binary correctness signal obtained via an LLM-as-judge protocol, which has shown to be correlated strongly with human judgment for free-form answer evaluation [50] (also see Section 4.3). Given the question, ground-truth answer, and predicted answer, the judge model returns a binary verdict based on semantic correctness rather than surface-level string matching. We use Qwen 2.5-14B [42] as the judge model and provide the prompt template in Appendix A.8.

**Mask Score** ( $S_m \in [0, 1]$ ) measures the fidelity of predicted segmentation masks as visual evidence. To handle single-instance, multi-instance, and hallucination samples uniformly,  $S_m$  is defined as:

$$S_m(P, G) = \begin{cases} 1 & \text{if } G = \emptyset \wedge P = \emptyset \\ 0 & \text{if } G = \emptyset \wedge P \neq \emptyset \\ \frac{1}{\max(|P|, |G|)} \sum_{(p,g) \in \mathcal{B}} \text{IoU}(p, g) & \text{otherwise} \end{cases} \quad (1)$$

where  $P$  is the set of predicted masks,  $G$  is the set of ground-truth masks, and  $\mathcal{B}$  is the bipartite matching between  $P$  and  $G$  obtained via the Hungarian algorithm [16]. The first case rewards correct predictions of no mask when none exists, corresponding to hallucination samples where the queried entity is absent from the scene. The second case penalizes spurious mask predictions when the ground truth is empty, reflecting a hallucination failure. The third case computes the mean IoU over the optimal matching, normalized by  $\max(|P|, |G|)$  to penalize both missed and spurious predictions.

**Joint Score (GROVE).** Directly multiplying  $S_a$  and  $S_m$  yields a degenerate metric: any sample with  $S_a = 0$  collapses to zero regardless of mask quality, potentially discarding meaningful grounding signals. To address this, we apply  $\epsilon$ -floor smoothing to both scores before computing the joint metric:

$$S'_a = \max(S_a, \epsilon) \quad (2)$$

$$S'_m = \max(S_m, \epsilon) \quad (3)$$

where  $\epsilon$  prevents score collapse while preserving sensitivity to partial correctness. We empirically choose a value of  $\epsilon = 0.1$ , which yields good score discriminability while balancing our desiderata of

Table 2: Per-task and overall results using VISTAQA. We report GROVE scores along with overall text accuracy ( $\mathcal{T}$ ) and overall mIoU ( $\mathcal{M}$ ) scores. <sup>†</sup> R-Sa2VA-Qwen3VL-4B-RL checkpoint.

Model	Per-task GROVE scores						Overall scores		
	Identification	Attribute	OCR	Spatial	Counting	Comparison	$\mathcal{T}$	$\mathcal{M}$	GROVE
LISA-7B [17]	15.16	16.92	12.44	15.29	16.56	16.23	7.26	17.81	15.47
SESAME-7B [40]	17.90	17.14	13.62	18.48	17.60	16.90	3.20	23.67	17.02
GLaMM-7B [29]	14.86	12.89	12.34	14.19	11.84	14.70	1.38	14.69	13.53
LaSagnA-7B [38]	13.31	12.03	11.04	13.23	11.14	13.05	0.43	10.74	12.35
UniPixel-7B [20]	22.24	28.29	22.19	19.90	15.36	26.34	21.26	20.43	22.39
Sa2VA-8B [44]	26.79	30.44	25.36	22.87	20.46	28.36	29.04	21.01	25.74
VRT-RL <sup>†</sup> [45]	34.92	28.74	27.43	24.44	29.94	28.01	36.30	24.25	29.02
TreeVGR-7B [35]	18.28	18.55	16.42	17.90	20.25	22.65	16.08	19.66	19.03
Uground-7B [27]	10.95	11.69	11.15	11.57	12.15	13.22	0.95	7.20	11.78
Qwen3-VL-4B-I + SAM3	50.36	47.46	40.96	36.32	45.52	38.43	53.15	39.91	43.30
Qwen3-VL-32B-I + SAM3	48.41	46.37	42.14	35.91	45.72	37.41	57.65	36.02	42.72
Gemini 3 + SAM3	43.10	40.11	42.55	33.53	42.81	35.84	62.32	34.99	39.63
GPT-5.4 + SAM3	48.22	40.43	41.33	35.62	47.06	35.86	53.50	39.26	41.50
GPT-5.4-T + SAM3	53.62	44.73	44.16	38.86	52.21	38.93	61.02	41.98	45.53

Table 3: Per-domain and hallucination results using VISTAQA. We report GROVE scores along with overall text accuracy ( $\mathcal{T}$ ) and overall mIoU ( $\mathcal{M}$ ) for hallucination and non-hallucination subsets. <sup>†</sup> denotes R-Sa2VA-Qwen3VL-4B-RL checkpoint.

Model	Per-domain GROVE scores						Hallucination scores			Non-Hallucination scores		
	Indoor	Outdoor	Math	AV	Rob.	Sci.	$\mathcal{T}$	$\mathcal{M}$	GROVE	$\mathcal{T}$	$\mathcal{M}$	GROVE
LISA-7B [17]	16.01	16.41	12.15	16.50	15.97	14.95	1.59	40.45	19.39	9.37	9.38	14.01
SESAME-7B [40]	17.20	17.68	11.05	20.77	15.92	17.97	9.87	61.46	30.04	0.71	9.59	12.17
GLaMM-7B [29]	12.82	13.75	11.13	15.70	13.43	13.72	0.32	4.14	10.96	1.78	18.62	14.48
LaSagnA-7B [38]	11.31	12.18	11.07	14.05	12.09	13.07	1.27	0.00	10.28	0.12	14.74	13.12
UniPixel-7B [20]	21.76	23.20	12.90	28.87	21.02	24.15	12.74	0.00	12.75	24.44	28.04	25.98
Sa2VA-8B [44]	22.64	24.03	14.87	36.87	25.10	28.09	7.32	0.00	11.58	37.13	28.84	31.01
VRT-RL <sup>†</sup> [45]	29.61	33.06	24.68	30.76	27.74	27.27	9.24	24.84	20.79	46.38	24.04	32.09
TreeVGR-7B [35]	18.41	20.45	12.70	23.51	19.76	17.78	26.43	24.52	22.66	12.22	17.85	17.68
Uground-7B [27]	11.32	10.74	10.78	11.79	13.40	12.38	2.55	14.01	14.03	0.36	4.66	10.94
Qwen3-VL-4B-I + SAM3	43.64	46.84	27.37	59.39	41.78	36.80	55.73	70.70	60.72	52.19	28.44	36.81
Qwen3-VL-32B-I + SAM3	44.27	47.63	23.23	58.40	40.09	37.85	61.78	55.73	56.41	56.11	28.68	37.63
Gemini 3 + SAM3	39.37	39.40	31.40	48.42	37.15	39.87	40.76	92.04	56.14	70.34	13.75	33.48
GPT-5.4 + SAM3	42.06	46.05	28.99	53.43	39.87	35.54	25.16	55.73	36.72	64.06	33.12	43.28
GPT-5.4-T + SAM3	45.39	45.92	41.51	53.18	47.01	39.24	39.17	67.20	47.89	69.16	32.59	44.65

joint sensitivity and graceful degradation (see section 4.3 and Appendix A.3). The per-sample score is then defined as the geometric mean of the smoothed scores:

$$\mathcal{S} = \sqrt{S'_a \cdot S'_m} \quad (4)$$

The geometric mean enforces joint competence by penalizing imbalance between the two axes [33], ensuring that strong performance on one axis cannot compensate for failure on the other.

**Benchmark Score.** The GROVE score with respect to  $N$  samples is computed as the mean of their per-sample scores:

$$\text{GROVE} = \frac{1}{N} \sum_{i=1}^N \mathcal{S}_i \quad (5)$$

where  $\mathcal{S}_i$  is the smoothed per-sample score (4).

## 4 Experiments

We evaluate various models spanning dedicated grounding and reasoning segmentation architectures, as well as pipeline approaches pairing frontier MLLMs with SAM3 [3]. All models are evaluated zero-shot without fine-tuning on VISTAQA and are provided with standardized output format instructions (Appendix A.9). All scores are reported as percentages. In addition to GROVE scores, for reference we include overall text accuracy ( $\mathcal{T}$ ) and overall mIoU ( $\mathcal{M}$ ), although these are not directly comparable with GROVE for reasons described in Appendix A.3. All evaluations are conducted on 4 NVIDIA GeForce RTX 4090 GPUs.

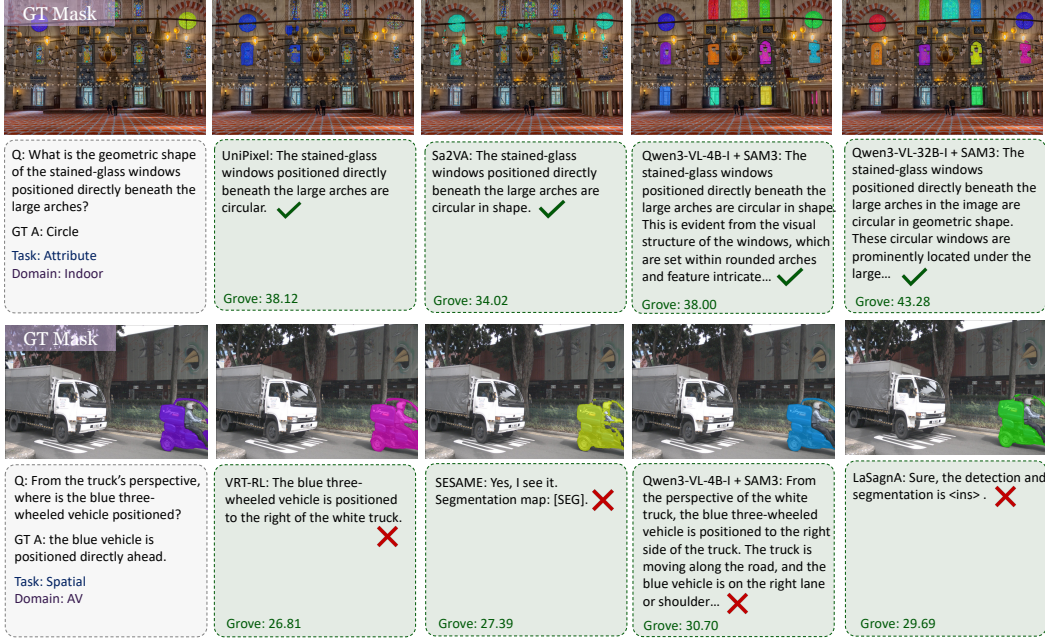


Figure 3: Illustration of the modality gap on VISTAQA. Top: correct answers ( $S_a = 1$ ) but inaccurate evidence ( $S_m < 0.2$ ). Bottom: accurate evidence ( $S_m > 0.7$ ) but incorrect answers ( $S_a = 0$ ). In both cases, partial correctness in a single modality yields low GROVE scores, highlighting the need for joint evaluation.

## 4.1 Results

Table 2 presents the overall performance of our chosen models using VISTAQA, along with a breakdown by task type. All models achieve low GROVE scores, with the strongest model, GPT-5.4-Thinking + SAM3 (GPT-5.4-T + SAM3), reaching only 45.53, highlighting the benchmark’s rigor in requiring simultaneous answer correctness and pixel-level evidence grounding. Among grounding-aware and reasoning segmentation models, VRT-RL achieves the best performance (29.02), followed by Sa2VA (25.74). Hybrid pipelines consistently outperform grounding models, with GPT-5.4-T + SAM3 achieving the highest overall score, followed by Qwen3-VL-4B-I+ SAM3. Crucially, a modality gap persists: while models may achieve relatively high text accuracy and mIoU mask scores, the joint GROVE remains low, indicating that correct answers and accurate evidence often occur on different samples. Across tasks, spatial reasoning and OCR emerge as the most challenging, reflecting their higher compositional and grounding demands.

Table 3 reports per-domain and hallucination breakdown results. Across domains, *Math* is consistently the most challenging for all model families, likely due to the abstraction required to ground symbolic reasoning in pixels. Hallucination samples reveal distinct failure modes. Several segmentation models predict masks even when no valid entity is present, whereas some hybrid pipelines tend to over-predict no masks, achieving high hallucination mask scores at the cost of reduced grounding quality on non-hallucination samples. Detailed per-task and per-domain text and mask score breakdowns are provided in Appendix A.2.

## 4.2 Qualitative Results

Figure 3 illustrates the modality gap across two representative failure modes. In the top row, models spanning grounding-specific (UniPixel, Sa2VA) and hybrid pipelines (Qwen3-VL-4B, Qwen3-VL-32B) correctly identify that the stained-glass windows are circular ( $S_a = 1$ ), yet segment irrelevant regions, resulting in low GROVE scores (34–43) despite perfect text accuracy. In the bottom row, all shown models accurately localize the blue vehicle ( $S_m > 0.7$ ) but misidentify its spatial relation to the truck, answering *right* instead of *ahead*, again yielding low GROVE scores (27–31) despite strong grounding. Crucially, both failure modes remain invisible under single-modality evaluation: the top

row would be deemed correct under text-only metrics, while the bottom row would score well under grounding-only metrics. A joint evaluation via GROVE reveals these failures. Additional qualitative results, including further examples illustrating GROVE behavior along with hallucination-aware cases are provided in Appendix A.5.

### 4.3 Discussion

Table 4: Agreement of various judges with human judgments.

Judge	Acc.	$\kappa$	$F_1$
Exact Match	0.520	0.000	0.000
Qwen2.5-14B	0.920	0.840	0.921
GPT-5.4	0.932	0.864	0.931

**LLM-as-Judge reliability for free-form text correctness.** To validate our LLM judge, we sample  $N = 250$  responses balanced across tasks, domains, models, and answer correctness. Table 4 reports accuracy, Cohen’s  $\kappa$  [7], and  $F_1$  for three evaluation methods against human judgments. Exact matching only achieves near-chance accuracy (52.0%, barely above the 50% random baseline for binary evaluation) and zero human agreement ( $\kappa = 0.00$ ), confirming that

lexical overlap is insufficient for evaluating free-form answers in VISTAQA. In contrast, Qwen2.5-14B demonstrates strong agreement with human judgments ( $\kappa = 0.840$ ), closely matching GPT-5.4 ( $\kappa = 0.864$ ), validating its use as a reliable and cost-efficient binary correctness judge.

**Sensitivity of GROVE to  $\epsilon$ .** GROVE uses the flooring parameter  $\epsilon$  to prevent score collapse while preserving sensitivity to sub-component variance. We adopt  $\epsilon = 0.1$  as this value yields the greatest score discriminability without compromising joint sensitivity. To validate our choice, we performed a sensitivity analysis with values of  $\epsilon \in \{0.01, 0.05, 0.1\}$ . Using these values, we found that model rankings are preserved at the overall score level (Spearman’s rank correlation  $\rho = 1.00$ ) and remain stable across task types and visual domains ( $\rho \geq 0.971$  per task,  $\rho \geq 0.974$  per domain), suggesting that GROVE is robust to the choice of  $\epsilon \in [0.01, 0.1]$ . The complete results are given in Tables 7 and 8 in Appendix A.3.

**Grounding Complexity.** Figure 4 compares overall mIoU ( $\mathcal{M}$ ) scores on samples requiring single- vs. multi-instance masks for representative models (full results in Appendix A.4). Most models degrade under multi-instance cases, highlighting simultaneous multi-region segmentation as a critical bottleneck. UniPixel and Sa2VA exhibit the most severe drops, despite achieving the strongest single-instance scores among grounding models. VRT-RL degrades least among grounding models ( $\Delta \approx -7$ ). Among hybrid pipelines, Gemini(G)3+SAM3 declines sharply ( $\Delta \approx -11$ ), whereas GPT-5.4+SAM3 maintains near-parity and slightly improves under multi-instance cases ( $\Delta \approx +1$ ). Qwen3-VL-32B+SAM3 also improves on multi-instance samples ( $\Delta \approx +4$ ), while Qwen3-VL-4B-I+SAM3 drops moderately, suggesting that model scale may help SAM3 for compositional grounding difficulty.

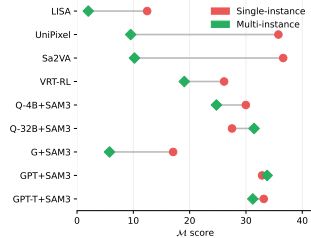


Figure 4: Single- vs. multi-instance  $\mathcal{M}$  scores.

## 5 Conclusion, Limitations, and Societal Impacts

**Conclusion.** We have introduced VISTAQA, a benchmark for the joint evaluation of free-form answer correctness and pixel-level evidence grounding in visual question answering. VISTAQA spans six task types and six visual domains with explicit hallucination-aware scenarios. To support rigorous evaluation, we have proposed GROVE, a unified metric that jointly assesses answer correctness and grounding fidelity via the geometric mean of smoothed per-axis scores. Comprehensive experiments across reasoning segmentation models, hybrid pipelines, and general-purpose MLLMs reveal that all evaluated models achieve low GROVE scores, exposing a fundamental gap between answer fluency and visual grounding fidelity that existing benchmarks fail to capture. We hope VISTAQA and GROVE serve as a foundation for future research in grounded multimodal evaluation.

**Limitations.** Due to the static nature of VISTAQA, video and multi-image grounding scenarios are not covered. Generating high-quality samples that simultaneously satisfy answer correctness, mask fidelity, and task diversity is inherently challenging and requires rigorous manual control at every stage of the pipeline. As a result, VISTAQA is limited to 1,157 high-quality samples despite significant annotation effort. This limitation stems from a circular dependency: the very models VISTAQA is designed to evaluate are not yet reliable enough to automate its construction.

**Societal Impacts.** VISTAQA is designed to improve the evaluation rigor of vision-language models, with direct benefits for transparency and reliability in safety-critical applications such as autonomous driving and robotics. The benchmark is constructed using images from publicly available datasets and contains no personally identifiable information. We have taken steps to mitigate annotation bias through multi-round human verification and cross-validation by independent annotators.

## References

- [1] Stanislaw Antol, Aishwarya Agrawal, Jiasen Lu, Margaret Mitchell, Dhruv Batra, C Lawrence Zitnick, and Devi Parikh. VQA: Visual question answering. In *Proceedings of the IEEE International Conference on Computer Vision*, pages 2425–2433, 2015.
- [2] Holger Caesar, Varun Bankiti, Alex H Lang, Sourabh Vora, Venice Erin Liong, Qiang Xu, Anush Krishnan, Yu Pan, Giancarlo Baldan, and Oscar Beijbom. nuScenes: A multimodal dataset for autonomous driving. In *Proceedings of the IEEE/CVF Conference on Computer Vision and Pattern Recognition*, pages 11621–11631, 2020.
- [3] Nicolas Carion, Laura Gustafson, Yuan-Ting Hu, Shoubhik Debnath, Ronghang Hu, Didac Suris, Chaitanya Ryali, Kalyan Vasudev Alwala, Haitham Khedr, Andrew Huang, et al. SAM 3: Segment anything with concepts. arXiv: 2511.16719, 2025.
- [4] Chongyan Chen, Samreen Anjum, and Danna Gurari. Grounding answers for visual questions asked by visually impaired people. In *Proceedings of the IEEE/CVF Conference on Computer Vision and Pattern Recognition*, pages 19098–19107, 2022.
- [5] Guo Chen, Zhiqi Li, Shihao Wang, Jindong Jiang, Yicheng Liu, Lidong Lu, De-An Huang, Wonmin Byeon, Matthieu Le, Max Ehrlich, Tong Lu, Limin Wang, Bryan Catanzaro, Jan Kautz, Andrew Tao, Zhiding Yu, and Guilin Liu. Eagle 2.5: Boosting long-context post-training for frontier vision-language models. In *The Thirty-ninth Annual Conference on Neural Information Processing Systems*, 2025.
- [6] Zhe Chen, Jiannan Wu, Wenhai Wang, Weijie Su, Guo Chen, Sen Xing, Muyan Zhong, Qinglong Zhang, Xizhou Zhu, Lewei Lu, et al. InternVL: Scaling up vision foundation models and aligning for generic visual-linguistic tasks. In *Proceedings of the IEEE/CVF Conference on Computer Vision and Pattern Recognition*, pages 24185–24198, 2024.
- [7] Jacob Cohen. A coefficient of agreement for nominal scales. *Educational and Psychological Measurement*, 20(1):37–46, 1960.
- [8] Shounak Datta and Dhanasekar Sundararaman. Evaluating hallucination in large vision-language models based on context-aware object similarities. arXiv: 2501.15046, 2025.
- [9] Chaoyou Fu, Peixian Chen, Yunhang Shen, Yulei Qin, Mengdan Zhang, Xu Lin, Jinrui Yang, Xiawu Zheng, Ke Li, Xing Sun, Yunsheng Wu, Rongrong Ji, Caifeng Shan, and Ran He. MME: A comprehensive evaluation benchmark for multimodal large language models. In *The Thirty-ninth Annual Conference on Neural Information Processing Systems, Datasets and Benchmarks Track*, 2025.
- [10] Google DeepMind. Gemini 3 Pro Model Card. Technical report, Google DeepMind, February 2025. URL <https://storage.googleapis.com/deepmind-media/Model-Cards/Gemini-3-Pro-Model-Card.pdf>.
- [11] Google DeepMind. Gemini 3.1 Pro Model Card. Technical report, Google DeepMind, February 2026. URL <https://storage.googleapis.com/deepmind-media/Model-Cards/Gemini-3-1-Pro-Model-Card.pdf>.
- [12] Yash Goyal, Tejas Khot, Douglas Summers-Stay, Dhruv Batra, and Devi Parikh. Making the V in VQA matter: Elevating the role of image understanding in visual question answering. In *Proceedings of the IEEE Conference on Computer Vision and Pattern Recognition*, pages 6904–6913, 2017.
- [13] Tianrui Guan, Fuxiao Liu, Xiyang Wu, Ruiqi Xian, Zongxia Li, Xiaoyu Liu, Xijun Wang, Lichang Chen, Furong Huang, Yaser Yacoob, et al. HallucinoBench: An advanced diagnostic suite for entangled language hallucination and visual illusion in large vision-language models. In *Proceedings of the IEEE/CVF Conference on Computer Vision and Pattern Recognition*, pages 14375–14385, 2024.
- [14] Alexander Khazatsky, Karl Pertsch, Suraj Nair, Ashwin Balakrishna, et al. DROID: A large-scale in-the-wild robot manipulation dataset. In *RSS 2024 Workshop: Data Generation for Robotics*, 2024.

- [15] Alexander Kirillov, Eric Mintun, Nikhila Ravi, Hanzi Mao, Chloe Rolland, Laura Gustafson, Tete Xiao, Spencer Whitehead, Alexander C Berg, Wan-Yen Lo, et al. Segment anything. In *Proceedings of the IEEE/CVF International Conference on Computer Vision*, pages 4015–4026, 2023.
- [16] Harold W. Kuhn. The Hungarian method for the assignment problem. *Naval Research Logistics Quarterly*, 2(1-2):83–97, 1955.
- [17] Xin Lai, Zhuotao Tian, Yukang Chen, Yanwei Li, Yuhui Yuan, Shu Liu, and Jiaya Jia. LISA: Reasoning segmentation via large language model. In *Proceedings of the IEEE/CVF Conference on Computer Vision and Pattern Recognition*, pages 9579–9589, 2024.
- [18] Xinzhuo Li, Adheesh Juvekar, Jiaxun Zhang, Xingyou Liu, Muntasir Wahed, Kiet A Nguyen, Yifan Shen, Tianjiao Yu, and Ismini Lourentzou. Counterfactual segmentation reasoning: Diagnosing and mitigating pixel-grounding hallucination. arXiv: 2506.21546, 2025.
- [19] Jiazhen Liu, Yuhan Fu, Ruobing Xie, Runquan Xie, Xingwu Sun, Fengzong Lian, Zhanhui Kang, and Xirong Li. PhD: A ChatGPT-prompted visual hallucination evaluation dataset. In *Proceedings of the Computer Vision and Pattern Recognition Conference*, pages 19857–19866, 2025.
- [20] Ye Liu, Zongyang Ma, Junfu Pu, Zhongang Qi, Yang Wu, Ying Shan, and Chang Wen Chen. UniPixel: Unified object referring and segmentation for pixel-level visual reasoning. In *The Thirty-ninth Annual Conference on Neural Information Processing Systems*, 2025.
- [21] Yuan Liu, Haodong Duan, Yuanhan Zhang, Bo Li, Songyang Zhang, Wangbo Zhao, Yike Yuan, Jiaqi Wang, Conghui He, Ziwei Liu, et al. MMBench: Is your multi-modal model an all-around player? In *European Conference on Computer Vision*, pages 216–233. Springer, 2024.
- [22] Pan Lu, Hritik Bansal, Tony Xia, Jiacheng Liu, Chunyuan Li, Hannaneh Hajishirzi, Hao Cheng, Kai-Wei Chang, Michel Galley, and Jianfeng Gao. MathVista: Evaluating mathematical reasoning of foundation models in visual contexts. In *The Twelfth International Conference on Learning Representations*, 2024.
- [23] Junhua Mao, Jonathan Huang, Alexander Toshev, Oana Camburu, Alan L Yuille, and Kevin Murphy. Generation and comprehension of unambiguous object descriptions. In *Proceedings of the IEEE Conference on Computer Vision and Pattern Recognition*, pages 11–20, 2016.
- [24] Ana-Maria Marcu, Long Chen, Jan Hünemann, Alice Karnsund, Benoit Hanotte, Prajwal Chidananda, Saurabh Nair, Vijay Badrinarayanan, Alex Kendall, Jamie Shotton, et al. LingoQA: Visual question answering for autonomous driving. In *European Conference on Computer Vision*, pages 252–269. Springer, 2024.
- [25] OpenAI. Update to GPT-5 System Card: GPT-5.2. Technical report, OpenAI, December 2025. URL [https://cdn.openai.com/pdf/3a4153c8-c748-4b71-8e31-aecbde944f8d/oai\\_5\\_2\\_system-card.pdf](https://cdn.openai.com/pdf/3a4153c8-c748-4b71-8e31-aecbde944f8d/oai_5_2_system-card.pdf).
- [26] OpenAI. GPT-5.4 Thinking System Card. Technical report, OpenAI, March 2026. URL <https://deploymentsafety.openai.com/gpt-5-4-thinking/gpt-5-4-thinking.pdf>.
- [27] Rui Qian, Xin Yin, Chuanhang Deng, Zhiyuan Peng, Jian Xiong, Wei Zhai, and Dejing Dou. UGround: Towards unified visual grounding with unrolled transformers. arXiv: 2510.03853, 2025.
- [28] Tianwen Qian, Jingjing Chen, Linhai Zhuo, Yang Jiao, and Yu-Gang Jiang. NuScenes-QA: A multi-modal visual question answering benchmark for autonomous driving scenario. In *Proceedings of the AAAI Conference on Artificial Intelligence*, volume 38, pages 4542–4550, 2024.
- [29] Hanoona Rasheed, Muhammad Maaz, Sahal Shaji, Abdelrahman Shaker, Salman Khan, Hisham Cholakkal, Rao M Anwer, Eric Xing, Ming-Hsuan Yang, and Fahad S Khan. GLaMM: Pixel grounding large multi-modal model. In *Proceedings of the IEEE/CVF Conference on Computer Vision and Pattern Recognition*, pages 13009–13018, 2024.
- [30] Aadarsh Sahoo and Georgia Gkioxari. Conversational image segmentation: Grounding abstract concepts with scalable supervision. arXiv: 2602.13195, 2026.
- [31] Tanik Saikh, Tirthankar Ghosal, Amish Mittal, Asif Ekbal, and Pushpak Bhattacharyya. ScienceQA: A novel resource for question answering on scholarly articles. *International Journal on Digital Libraries*, 23(3):289–301, 2022.
- [32] Chonghao Sima, Katrin Renz, Kashyap Chitta, Li Chen, Hanxue Zhang, Chengen Xie, Jens Beißwenger, Ping Luo, Andreas Geiger, and Hongyang Li. DriveLM: Driving with graph visual question answering. In *European Conference on Computer Vision*, pages 256–274. Springer, 2024.

- [33] J. Michael Steele. *The Cauchy-Schwarz Master Class*. Cambridge University Press, 2004.
- [34] An Vo, Khai-Nguyen Nguyen, Mohammad Reza Taesiri, Vy Tuong Dang, Anh Totti Nguyen, and Daeyoung Kim. Vision language models are biased. In *The Fourteenth International Conference on Learning Representations*, 2026. URL <https://openreview.net/forum?id=DG4S201GQA>.
- [35] Haochen Wang, Xiangtai Li, Zilong Huang, Anran Wang, Jiacong Wang, Tao Zhang, Sule Bai, Zijian Kang, Jiashi Feng, Wang Zhuochen, et al. Traceable evidence enhanced visual grounded reasoning: Evaluation and method. In *The Fourteenth International Conference on Learning Representations*, 2026.
- [36] Weiyun Wang, Zhangwei Gao, Lixin Gu, Hengjun Pu, Long Cui, Xingguang Wei, Zhaoyang Liu, Linglin Jing, Shenglong Ye, Jie Shao, et al. InternVL3.5: Advancing open-source multimodal models in versatility, reasoning, and efficiency. arXiv: 2508.18265, 2025.
- [37] Yimu Wang, Mozghan Nasr Azadani, Sean Sedwards, and Krzysztof Czarnecki. Hawaii: Hierarchical visual knowledge transfer for efficient vision-language models. In *The Thirty-ninth Annual Conference on Neural Information Processing Systems*, 2025.
- [38] Cong Wei, Haoxian Tan, Yujie Zhong, Yujiu Yang, and Lin Ma. LaSagnA: Language-based segmentation assistant for complex queries. arXiv: 2404.08506, 2024.
- [39] Penghao Wu and Saining Xie. V\*: Guided visual search as a core mechanism in multimodal LLMs. In *Proceedings of the IEEE/CVF Conference on Computer Vision and Pattern Recognition*, pages 13084–13094, 2024.
- [40] Tsung-Han Wu, Giscard Biamby, David Chan, Lisa Dunlap, Ritwik Gupta, Xudong Wang, Joseph E Gonzalez, and Trevor Darrell. See, say, and segment: Teaching LMMs to overcome false premises. In *Proceedings of the IEEE/CVF Conference on Computer Vision and Pattern Recognition*, pages 13459–13469, 2024.
- [41] Cilin Yan, Haochen Wang, Shilin Yan, Xiaolong Jiang, Yao Hu, Guoliang Kang, Weidi Xie, and Efstratios Gavves. VISA: Reasoning video object segmentation via large language models. In *European Conference on Computer Vision*, pages 98–115. Springer, 2024.
- [42] An Yang, Anfeng Li, Baosong Yang, Beichen Zhang, Binyuan Hui, Bo Zheng, Bowen Yu, Chang Gao, Chengen Huang, Chenxu Lv, et al. Qwen3 technical report. arXiv: 2505.09388, 2025.
- [43] Licheng Yu, Patrick Poirson, Shan Yang, Alexander C Berg, and Tamara L Berg. Modeling context in referring expressions. In *European Conference on Computer Vision*, pages 69–85. Springer, 2016.
- [44] Haobo Yuan, Xiangtai Li, Tao Zhang, Yueyi Sun, Zilong Huang, Shilin Xu, Shunping Ji, Yunhai Tong, Lu Qi, Jiashi Feng, et al. Sa2VA: Marrying SAM2 with MLLM for dense grounded understanding of images and videos. arXiv: 2501.04001, 2025.
- [45] Haobo Yuan, Yueyi Sun, Yanwei Li, Tao Zhang, Xueqing Deng, Henghui Ding, Lu Qi, Anran Wang, Xiangtai Li, and Ming-Hsuan Yang. Visual reasoning tracer: Object-level grounded reasoning benchmark. arXiv: 2512.05091, 2025.
- [46] Xiang Yue, Yuansheng Ni, Kai Zhang, Tianyu Zheng, Ruoqi Liu, Ge Zhang, Samuel Stevens, Dongfu Jiang, Weiming Ren, Yuxuan Sun, et al. MMMU: A massive multi-discipline multimodal understanding and reasoning benchmark for expert AGI. In *Proceedings of the IEEE/CVF Conference on Computer Vision and Pattern Recognition*, pages 9556–9567, 2024.
- [47] Xiang Yue, Tianyu Zheng, Yuansheng Ni, Yubo Wang, Kai Zhang, Shengbang Tong, Yuxuan Sun, Botao Yu, Ge Zhang, Huan Sun, et al. MMMU-Pro: A more robust multi-discipline multimodal understanding benchmark. In *Proceedings of the 63rd Annual Meeting of the Association for Computational Linguistics.*, pages 15134–15186, 2025.
- [48] Tao Zhang, Xiangtai Li, Hao Fei, Haobo Yuan, Shengqiong Wu, Shunping Ji, Chen Change Loy, and Shuicheng Yan. Omg-llava : Bridging image-level, object-level, pixel-level reasoning and understanding. In *Advances in Neural Information Processing Systems*, volume 37, pages 71737–71767, 2024.
- [49] Zongmeng Zhang, Wengang Zhou, Jie Zhao, and Houqiang Li. Robust multimodal large language models against modality conflict. In *International Conference on Machine Learning*, pages 77233–77253. PMLR, 2025.
- [50] Lianmin Zheng, Wei-Lin Chiang, Ying Sheng, Siyuan Zhuang, Zhanghao Wu, Yonghao Zhuang, Zi Lin, Zhuohan Li, Dacheng Li, Eric Xing, et al. Judging LLM-as-a-judge with MT-Bench and Chatbot Arena. In *Advances in Neural Information Processing Systems*, volume 36, pages 46595–46623, 2023.

## A Appendix

- A.1: Tasks
- A.2: Additional Results
- A.3: Choice of  $\epsilon$
- A.4: Grounding Complexity
- A.5: Additional Qualitative Results
- A.6: Examples of Failure Cases in VQA Generation
- A.7: Prompts for Generating VQA Tasks
- A.8: Prompt for LLM-as-a-Judge Evaluation of Answer Correctness
- A.9: Structured Output Format

### A.1 Tasks

VISTAQA defines six task types that reflect the diverse reasoning demands of VQA, ranging from direct perception to multi-hop reasoning. Each task requires models to jointly produce a correct free-form answer and a segmentation mask that explicitly grounds the prediction in the relevant image region. The tasks include *Identification*, *Attribute*, *OCR*, *Spatial*, *Counting*, and *Comparison*, each described below.

1. **Identification** evaluates the ability to recognize and name objects, entities, or scene elements present in the image. The task requires precise localization of the target and accurate category-level or instance-level recognition, particularly in cluttered or multi-object scenes where discriminative grounding is essential.
2. **Attribute** evaluates the ability to identify and describe specific properties of objects or regions, including color, shape, texture, and fine-grained appearance characteristics. Success requires attention to subtle visual details and accurate association of properties with the correct image region, particularly when multiple objects share similar features.
3. **OCR** evaluates the ability to detect, read, and interpret text present in the scene, requiring tight integration of localization and text recognition. This task is particularly challenging in domains where text appears at varying scales, orientations, or under partial occlusion, and where the answer must be grounded in the specific image region containing the relevant text.
4. **Spatial** evaluates the ability to interpret positional and geometric relationships between objects or regions in the scene, including absolute and relative positions, directional relationships, and proximity. The task requires integrating localization with relational reasoning to produce answers grounded in the correct spatial configuration.
5. **Counting** evaluates the ability to enumerate instances of a specified category within the image, requiring systematic localization of all relevant regions and aggregation of evidence across the scene. This task is particularly demanding in dense or occluded scenes where individual instances are difficult to discriminate.
6. **Comparison** evaluates the ability to reason about differences or similarities between two or more objects, regions, or attributes within the image. Correct answers require localizing relevant region, and performing relational inference over the evidence.

### A.2 Additional Results

Table 5 reports overall text and mask scores per task type. While pipeline models achieve strong text scores, particularly on OCR tasks (*e.g.*, Gemini 3 + SAM3 reaches 72.83), their corresponding mask scores remain low. Crucially, high text and mask scores do not necessarily reflect correct performance on the same samples: a model may answer the textual query correctly on one subset of samples while producing accurate masks on an entirely different subset. This decoupling is precisely why GROVE, reported in the main paper, is needed as a joint metric that rewards models only when both modalities are correct for the same instance.

Table 6 reveals the same pattern across all six domains, where dedicated grounding and segmentation models consistently underperform hybrid pipeline approaches. AV scenes yield the highest text scores for pipeline models, yet mask scores there remain moderate, while Math is the hardest domain across both modalities for all model families. Crucially, the persistent text-mask gap across all domains reinforces that reporting either score in isolation paints an incomplete and potentially misleading picture of model capability, further validating GROVE as the primary evaluation metric.

Table 5: Detailed per-task results on VISTAQA. We report overall text accuracy ( $\mathcal{T}$ ) and overall mIoU ( $\mathcal{M}$ ) per task. <sup>†</sup> R-Sa2VA-Qwen3VL-4B-RL checkpoint.

Model	Identification		Attribute		OCR		Spatial		Counting		Comparison	
	$\mathcal{T}$	$\mathcal{M}$	$\mathcal{T}$	$\mathcal{M}$	$\mathcal{T}$	$\mathcal{M}$	$\mathcal{T}$	$\mathcal{M}$	$\mathcal{T}$	$\mathcal{M}$	$\mathcal{T}$	$\mathcal{M}$
LISA-7B [17]	7.48	16.37	12.04	19.85	2.89	9.24	5.03	19.34	8.51	22.05	7.29	19.36
SESAME-7B [40]	3.74	26.80	2.62	26.32	2.31	12.98	5.03	23.57	3.19	25.59	2.08	25.40
GLaMM-7B [29]	2.34	19.72	1.57	11.63	0.58	10.51	1.01	17.27	0.53	9.27	2.08	18.51
LaSagnA-7B [38]	0.00	15.41	0.00	9.80	0.58	4.96	1.01	13.82	0.53	6.03	0.52	13.10
UniPixel-7B [20]	17.76	24.77	30.89	25.05	32.95	13.72	11.56	23.21	10.64	9.87	25.52	24.53
Sa2VA-8B [44]	27.10	26.29	33.51	26.94	41.62	12.11	17.59	22.86	25.53	11.84	30.73	24.32
VRT-RL <sup>†</sup> [45]	39.25	30.32	39.79	23.22	38.15	24.75	28.64	19.82	28.72	27.94	43.23	19.06
TreeVGR-7B [35]	11.21	23.15	14.66	20.46	9.25	18.75	12.56	17.79	18.62	19.43	30.21	17.96
Uground-7B [27]	0.47	4.70	1.05	5.99	1.16	4.45	0.50	6.74	0.53	10.38	2.08	11.03
Qwen3-VL-4B-I + SAM3	54.67	48.53	58.12	43.89	63.01	31.47	41.21	37.95	46.28	47.13	56.77	28.92
Qwen3-VL-32B-I + SAM3	58.88	43.61	60.73	42.10	68.79	29.70	48.74	27.43	47.34	47.83	62.50	24.54
Gemini 3 + SAM3	63.55	39.56	60.21	39.51	72.83	33.54	49.75	34.01	61.70	32.19	67.19	30.48
GPT-5.4 + SAM3	57.48	47.98	49.21	42.52	65.32	32.54	47.24	30.84	46.28	53.98	56.25	26.67
GPT-5.4-T + SAM3	63.08	54.65	59.16	43.55	73.41	33.20	51.26	38.59	55.85	51.85	64.58	28.09

Table 6: Detailed per-domain results on VISTAQA. We report overall text accuracy ( $\mathcal{T}$ ) and overall mIoU ( $\mathcal{M}$ ) per domain. <sup>†</sup> R-Sa2VA-Qwen3VL-4B-RL checkpoint.

Model	Indoor		Outdoor		Math		AV		Robotics		Science	
	$\mathcal{T}$	$\mathcal{M}$	$\mathcal{T}$	$\mathcal{M}$	$\mathcal{T}$	$\mathcal{M}$	$\mathcal{T}$	$\mathcal{M}$	$\mathcal{T}$	$\mathcal{M}$	$\mathcal{T}$	$\mathcal{M}$
LISA-7B [17]	6.34	19.41	11.22	18.56	2.67	8.74	11.88	18.18	6.00	21.32	4.41	18.33
SESAME-7B [40]	3.90	22.40	4.59	23.41	0.67	4.58	4.95	35.24	2.00	22.18	2.45	29.23
GLaMM-7B [29]	2.44	9.12	2.04	15.35	0.00	6.50	1.98	23.83	1.00	14.53	0.49	16.78
LaSagnA-7B [38]	0.00	6.77	1.53	8.87	0.67	5.99	0.50	17.40	0.00	9.90	0.00	14.24
UniPixel-7B [20]	26.34	15.43	23.47	19.66	3.33	11.46	29.21	29.56	14.50	21.56	25.98	22.65
Sa2VA-8B [44]	29.27	15.59	31.63	17.60	10.00	9.65	44.55	32.70	26.00	21.91	27.94	25.63
VRT-RL <sup>†</sup> [45]	40.98	21.69	39.80	27.89	28.00	18.75	41.09	27.30	29.50	22.88	36.27	25.71
TreeVGR-7B [35]	16.59	16.51	23.47	20.13	4.67	9.15	21.78	27.83	14.00	24.70	13.24	17.08
Uground-7B [27]	0.49	5.92	0.51	3.45	0.00	4.80	0.99	7.41	1.50	12.31	1.96	8.64
Qwen3-VL-4B-I + SAM3	52.20	39.45	58.67	42.21	35.33	22.50	72.28	55.33	45.00	43.01	50.98	32.67
Qwen3-VL-32B-I + SAM3	61.95	34.83	65.31	39.47	32.67	17.18	76.73	49.55	44.00	41.26	58.82	29.22
Gemini 3 + SAM3	62.93	34.79	63.27	33.24	55.33	22.97	67.33	46.48	51.50	37.20	71.57	32.22
GPT-5.4 + SAM3	62.93	39.00	63.27	39.74	55.33	23.30	67.33	51.67	51.50	45.37	71.57	32.52
GPT-5.4-T + SAM3	64.88	39.58	65.31	41.55	58.00	33.37	68.81	48.89	48.00	50.15	60.29	36.31

### A.3 Choice of $\epsilon$

The flooring parameter  $\epsilon$  in GROVE sets the minimum score assigned to failed predictions, preventing score collapse during aggregation. More specifically, this parameter prevents the joint score from collapsing to zero when one component fails, preserving the ability to discriminate models based on the quality of the other component. We perform a sensitivity analysis on  $\epsilon$  with results shown in Tables 7 and 8 for  $\epsilon \in \{0.01, 0.05, 0.1\}$ . We see that GROVE exhibits strong robustness to the choice of the flooring parameter  $\epsilon$ . While absolute GROVE scores increase monotonically with larger  $\epsilon$ , model rankings are fully preserved across all settings ( $\rho = 1.00$ ), suggesting that the relative ordering of models is invariant for  $\epsilon \in [0.01, 0.1]$ .

This stability is further supported by the correlation analysis in Table 8. At finer granularity, per-task and per-domain correlations remain high ( $\rho \geq 0.971$ ). Accordingly, we adopt  $\epsilon = 0.1$ , which provides the highest score discriminability while preserving ranking consistency.

While larger values of  $\epsilon$  monotonically increase absolute GROVE scores and preserve model rankings (as shown in Table 7), setting  $\epsilon > 0.1$  progressively undermines the metric’s core desideratum of *joint sensitivity*. To see why, consider the extreme case  $\epsilon \rightarrow 1$ : both  $S'_a$  and  $S'_m$  collapse toward 1 regardless of actual model performance, rendering GROVE uninformative. More concretely, at  $\epsilon = 0.1$  a model that fails entirely on one modality (e.g.,  $S_a = 0$ ) receives a floored score of  $S'_a = 0.1$ , contributing a joint score of at most  $\sqrt{0.1 \times 1} \approx 0.316$  — a meaningful penalty. At  $\epsilon = 0.3$ , the same fully-failing model on one modality would receive  $\sqrt{0.3 \times 1} \approx 0.548$ , which reduces the headroom to distinguish it from models with genuine partial competence. We therefore choose  $\epsilon = 0.1$  as the largest value that preserves meaningful penalization of single-modality failures while avoiding score collapse in the other direction.

The use of  $\epsilon$ -flooring ensures that samples with one failed component do not collapse to zero, while still penalizing the lack of joint correctness. This can result in seemingly anomalous results, where per-sample scores (4) exceed one or both of the individual components and the GROVE score (5) is not bounded by the dataset-level averages of its marginals. This is intentional: GROVE deliberately reflects a softened measure of joint alignment.

Table 7: GROVE scores and ranks for all models across  $\epsilon \in \{0.01, 0.05, 0.1\}$ . Rankings are fully preserved across all settings ( $\rho = 1.00$ ), with  $\epsilon = 0.1$  yielding the highest discriminability. <sup>†</sup> R-Sa2VA-Qwen3VL-4B-RL checkpoint.

Model	GROVE Score			Rank		
	$\epsilon = 0.01$	$\epsilon = 0.05$	$\epsilon = 0.1$	$\epsilon = 0.01$	$\epsilon = 0.05$	$\epsilon = 0.1$
LISA-7B [17]	3.61	9.60	15.47	11	11	11
SESAME-7B [40]	5.87	11.44	17.02	10	10	10
GLaMM-7B [29]	2.93	8.15	13.53	12	12	12
LaSagnA-7B [38]	2.37	7.16	12.35	13	13	13
UniPixel-7B [20]	12.02	17.24	22.39	8	8	8
Sa2VA-8B [44]	16.02	20.88	25.74	7	7	7
VRT-RL <sup>†</sup> [45]	17.93	23.70	29.02	6	6	6
TreeVGR-7B [35]	7.54	13.51	19.03	9	9	9
UGround-7B [27]	2.13	6.64	11.78	14	14	14
Qwen3-VL-4B + SAM3	34.14	38.98	43.30	2	2	2
Qwen3-VL-32B + SAM3	33.51	38.40	42.72	3	3	3
Gemini-3-Flash + SAM3	25.49	33.30	39.63	5	5	5
GPT-no-thinking + SAM3	31.61	36.90	41.50	4	4	4
GPT-thinking + SAM3	35.86	41.08	45.53	1	1	1

Table 8: Spearman  $\rho$  between GROVE rankings across  $\epsilon$  values at overall, per-task, and per-domain granularity. All correlations are statistically significant.

Granularity		$\epsilon_{0.1}$ vs $\epsilon_{0.05}$	$\epsilon_{0.1}$ vs $\epsilon_{0.01}$	$\epsilon_{0.05}$ vs $\epsilon_{0.01}$
Overall		1.000	1.000	1.000
Task	Identification	1.000	0.996	0.996
	Attribute	0.996	0.993	0.996
	OCR	0.993	0.971	0.986
	Spatial	1.000	0.996	0.996
	Counting	0.989	0.986	0.996
	Comparison	0.996	0.986	0.993
Domain	Indoor	0.996	0.996	1.000
	Outdoor	1.000	1.000	1.000
	Math	0.988	0.974	0.982
	AV	0.996	0.993	0.996
	Robotics	0.993	0.993	1.000
	Science	0.996	0.968	0.975

#### A.4 Grounding Complexity

Figure 5 extends the analysis in the main paper to all 14 models, reporting overall mask scores for single- and multi-instance samples separately. The degradation pattern is consistent across model families: grounding-specific models show the largest absolute drops, with UniPixel and Sa2VA collapsing by over 26 points, while TreeVGR and VRT-RL are comparatively robust. Among hybrid pipelines, Gemini3+SAM3 degrades sharply despite strong overall performance, whereas GPT-5.4+SAM3 and Qwen3-VL-32B+SAM3 improve their mask scores under multi-instance grounding, suggesting that model scale and reasoning ability partially compensate for the added segmentation complexity. These results confirm that multi-instance grounding represents a fundamentally harder challenge than single-instance localization across all evaluated model families.

#### A.5 Additional Qualitative Results

Figures 6–10 present qualitative examples illustrating the four outcome combinations captured by GROVE, along with hallucination-aware samples. Figure 6 shows cases where both the textual answer and the evidence mask are correct, yielding high GROVE scores (*e.g.*, GROVE  $\approx$  86–99). These examples demonstrate that when

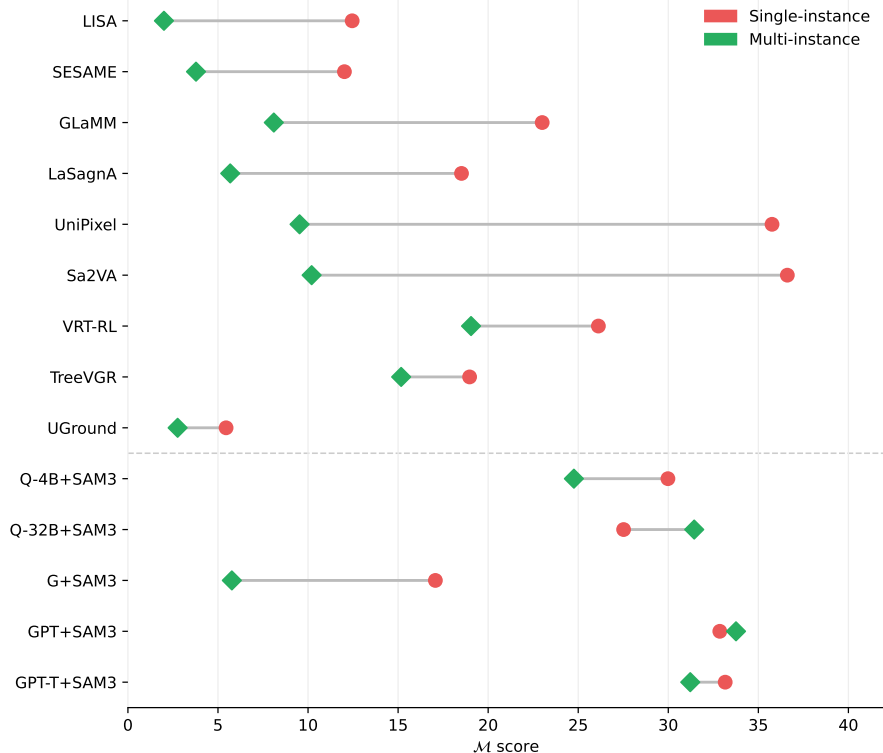


Figure 5: Single- vs. multi-instance overall mask scores for all 14 models. The dashed line separates grounding-specific models (above) from hybrid pipelines (below).

models correctly answer the question and ground the target evidence precisely, GROVE effectively rewards joint alignment across diverse tasks and domains, including outdoor scenes, robotics, and indoor environments.

Figure 7 highlights a key failure mode: the textual answer is correct but the evidence mask is misaligned, resulting in relatively low GROVE scores despite accurate reasoning. This reflects cases where models answer correctly but fail to localize the relevant evidence, confirming that GROVE penalizes ungrounded correct answers. Conversely, Figure 8 shows cases where the mask quality is high but the textual answer is incorrect, models segment the correct region but draw wrong conclusions, also yielding relatively low GROVE scores.

Figure 9 presents the worst-case scenario, where both the answer and the mask are incorrect, leading to the lowest GROVE scores ( $GROVE \approx 10-13$ ). Notably, these scores do not collapse to zero due to  $\epsilon$ -flooring, as discussed in Section 4.1. Finally, Figure 10 illustrates hallucination-aware samples where the ground-truth mask is empty. Models that correctly recognize the absence of the queried entity produce an empty mask, while those that hallucinate a non-empty mask or provide an incorrect answer are penalized.

Overall, these examples demonstrate that GROVE captures a richer and more reliable signal than either text accuracy or mask quality alone.

## A.6 Examples of Failure Cases in VQA Generation

Figures 11 present representative failure cases in QA generation using GPT-5.2 [25] and Gemini 3 pro [10], highlighting the limitations of fully automated pipelines and the necessity of human verification. As shown, models may produce incorrect answers in counting such as miscounting cushions, dice pips, or food items, generate ambiguous or wrong questions where the answer is encoded in the questions themselves. These examples demonstrate that QA generation errors arise at both the question and answer levels.

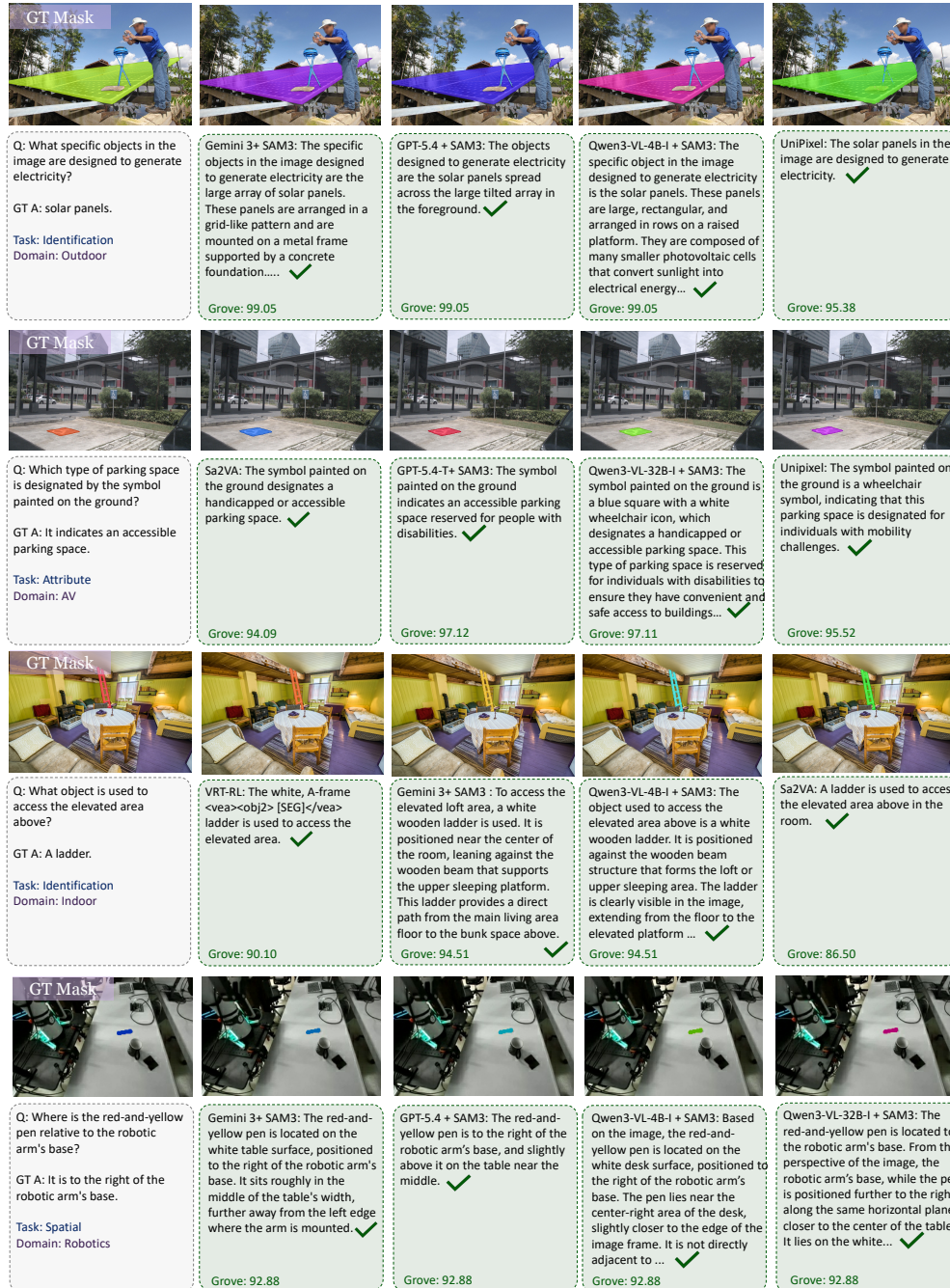


Figure 6: Qualitative examples where the textual answer is correct ( $S_a = 1$ ) and the evidence mask achieves high overlap with the ground-truth annotation, yielding high GROVE scores.

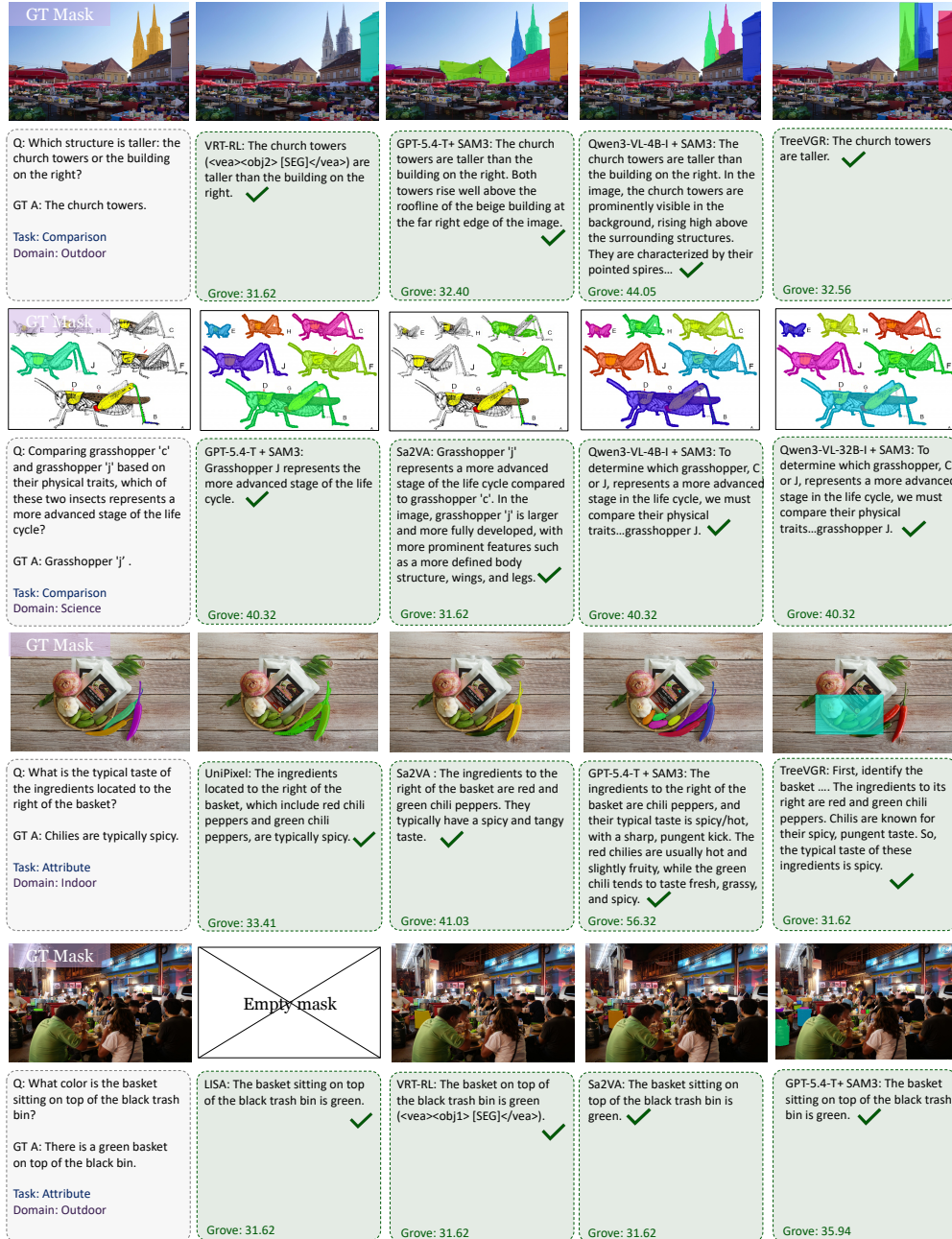


Figure 7: Qualitative examples where the textual answer is correct ( $S_a = 1$ ) and the evidence mask achieves **low** overlap with the ground-truth annotation, yielding low GROVE scores.

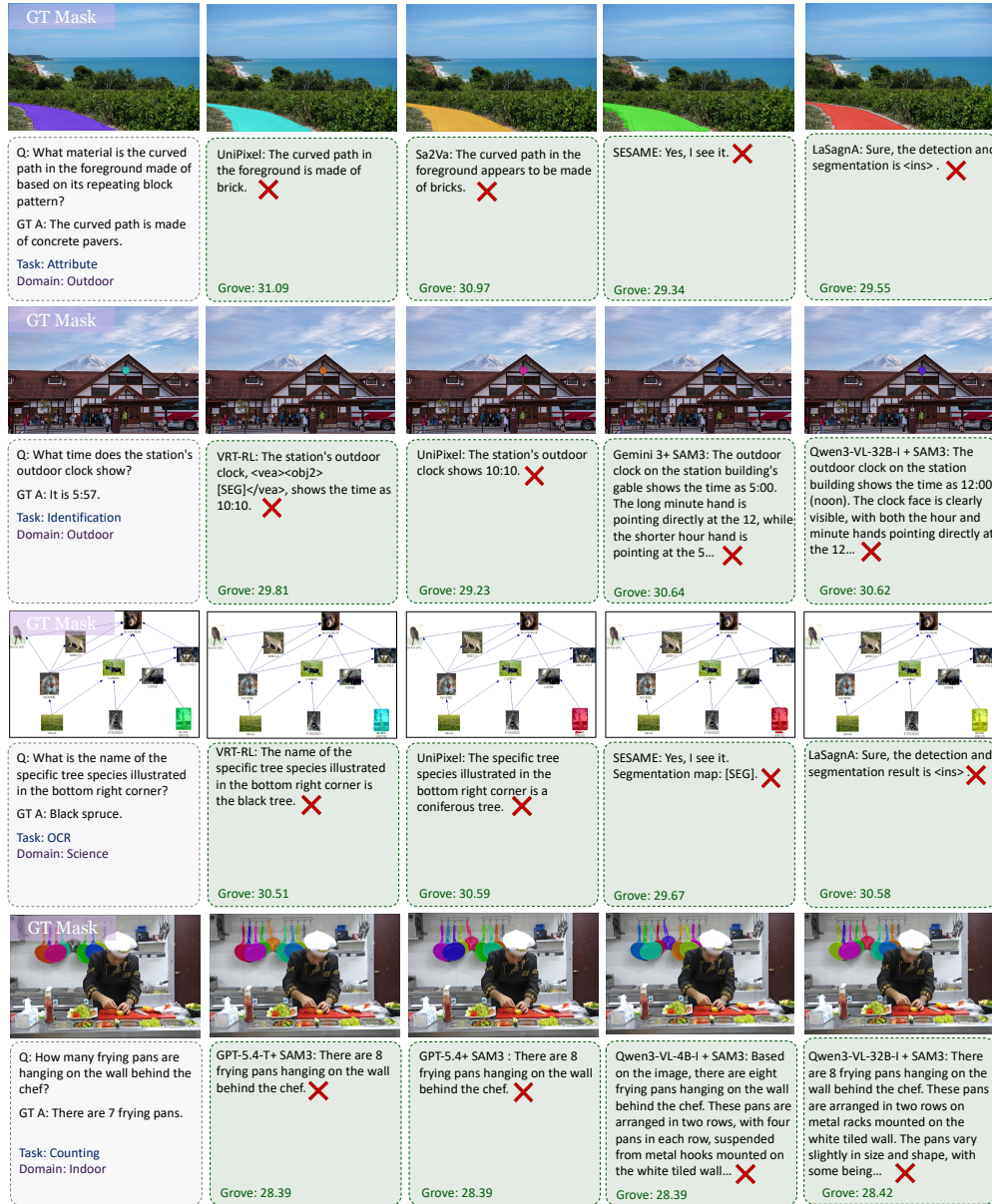


Figure 8: Qualitative examples where the textual answer is incorrect ( $S_a = 0$ ) and the evidence mask achieves high overlap with the ground-truth annotation, yielding low GROVE scores.

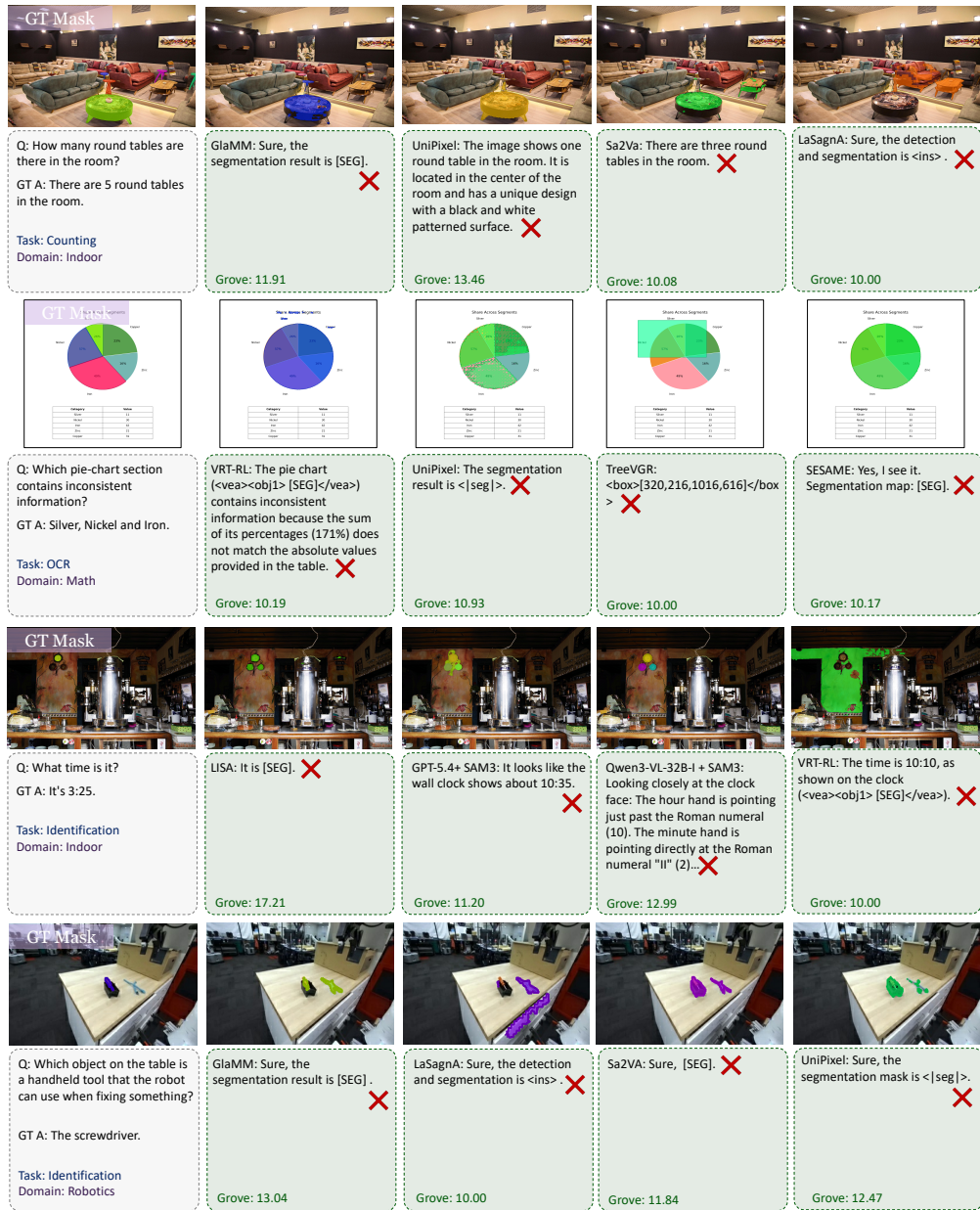


Figure 9: Qualitative examples where the textual answer is incorrect ( $S_a = 0$ ) and the evidence mask achieves low overlap with the ground-truth annotation, yielding low GROVE scores.








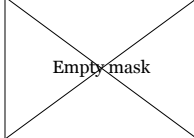

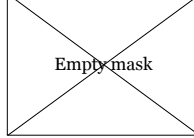

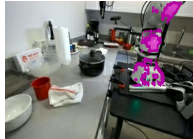
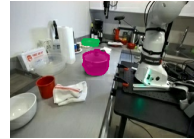
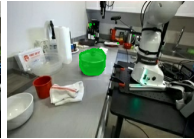


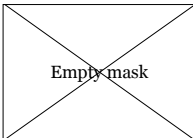

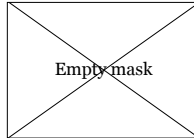

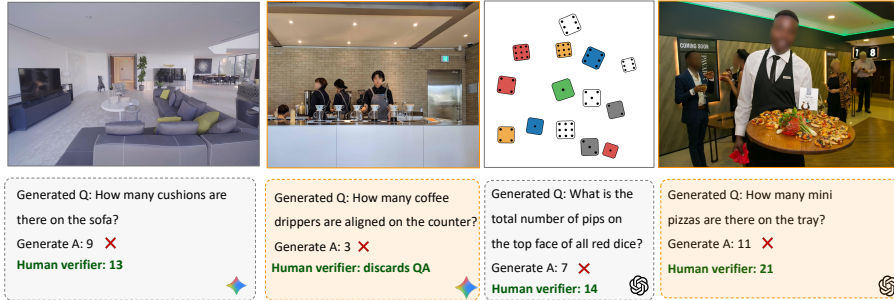
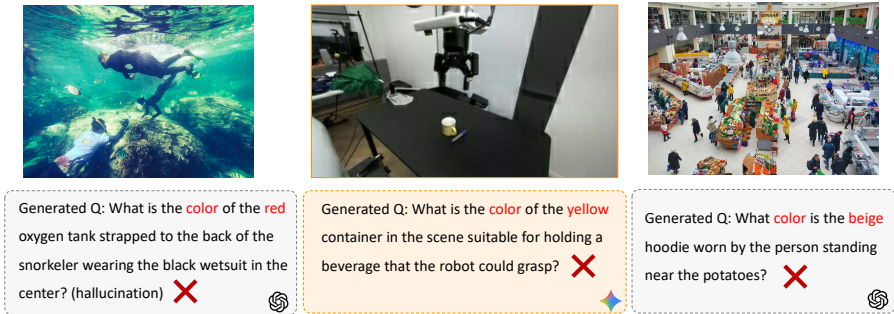
				
<p>Q: According to the departure board, what is the gate number for Toronto?</p> <p>GT A: There is no information about Toronto on the board. GT mask: Empty.</p> <p>Task: OCR Domain: Indoor</p>	<p>LISA: It is [SEG]. ❌</p>	<p>TreeVGR: The board lists train destinations and their corresponding gates. &lt;box&gt;[872,712,1424,912]&lt;/box&gt; shows that the train to Toronto has a gate number of 17. So the gate number for Toronto is 17. ❌</p>	<p>Qwen3-VL-32B-I + SAM3: Based on the departure board visible in the image, there is no train listed for Toronto. The board displays departures for VIA Rail Canada, with destinations including Ottawa, Montreal, and Windsor. The gate numbers listed are for these destinations but Toronto is not among the listed destinations on this board. ✓</p>	<p>VRT-RL: The gate number for Toronto, as shown on the departure board (&lt;vea&gt;&lt;obj1&gt;[SEG]&lt;/vea&gt;), is 1700. ❌</p>
				
<p>Q: How many street performers are wearing bright yellow neon vests while performing in the center of the square?</p> <p>GT A: There are no performers wearing bright yellow neon vests. GT mask: Empty</p> <p>Task: Counting Domain: Outdoor</p>	<p>Glamm: Sure, the segmentation result is [SEG]. ❌</p>	<p>Gemini 3+ SAM3: Based on the image, there are no street performers wearing bright yellow neon vests in the center of the square. The only clearly visible street performer is a man sitting on the left side of the square playing an acoustic guitar. ✓</p>	<p>TreeVGR: There are no street performers wearing bright yellow neon vests in the center of the square. The street performer visible in the image is a man playing a guitar and singing, and he is not wearing a neon vest. The question asks for the number of such performers, and since there are none, the answer is zero. ✓</p>	<p>GPT-5.4-T + SAM3: There are 0 street performers wearing bright yellow neon vests while performing in the center of the square. The only clearly visible performer is the musician in the lower-left foreground, and he is not wearing a bright yellow neon vest. ✓</p>
				
<p>Q: If the robot reaches for the object to the left of the knife from camera's perspective, what will it pick?</p> <p>GT A: There is no knife on the counter. GT mask: Empty</p> <p>Task: Spatial Domain: Robotics</p>	<p>LaSagNA: Sure, the detection and segmentation result is &lt;ins&gt;. ❌</p>	<p>GPT-5.4-T + SAM3: It would pick the black pot, which is to the left of the knife from the camera's perspective. ❌</p>	<p>Unipixel: The target is &lt; seg &gt;. ❌</p>	<p>VRT-RL: The robot would pick up the red bucket. ❌</p>
				
<p>Q: Comparing the red motorcycle and the yellow car, which is parked nearer to the barrier arm?</p> <p>GT A: there is no red motorcycle visible in the image, so this comparison cannot be made. GT mask: Empty</p> <p>Task: Comparison Domain: AV</p>	<p>Qwen3-VL-48-I + SAM3: Since there is no red motorcycle in the image, a comparison between the red motorcycle and the yellow car is not possible. The yellow car is the only vehicle in proximity to the barrier arm. ✓</p>	<p>GPT-5.4-T + SAM3: The yellow car is parked nearer. ❌</p>	<p>Gemini 3+ SAM3: : Based on the image, the yellow car is parked much nearer to the barrier arm than the red motorcycle. The yellow car is positioned directly next to the barrier arm on the right side of the road, while the red motorcycle is parked further back in the distance, near the guard house area on the left side of the road. ❌</p>	<p>Sa2VA: The yellow car is parked nearer to the barrier arm compared to the red motorcycle. ✓</p>

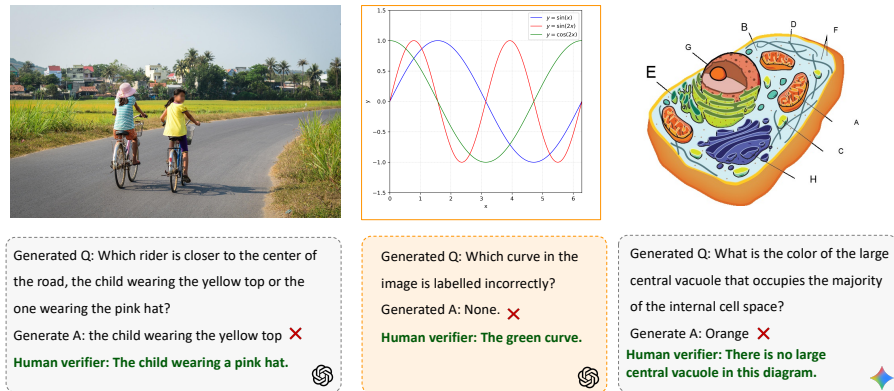
Figure 10: Examples of various models' outputs on hallucination-aware samples, where the ground-truth mask is empty.



(a) Counting-related failures in QA generation.



(b) QA generation failures where the answer is implicitly contained in the question.



(c) QA generation failures due to incorrect answers.

Figure 11: Failure cases in automated QA generation, highlighting the need for human verification

## A.7 Prompts for Generating VQA Tasks

### Template Prompt for Attribute Task

The primary goal of this task is to generate challenging compositional and multi-hop VQA questions for attribute reasoning. Analyze the given image carefully and generate five diverse attribute-based questions, each paired with a concise answer. The questions should rely on attributes such as color, size, shape, texture, behavior, or similar properties.

### Template Prompt for OCR Task

The primary goal of this task is to generate high-quality VQA questions for OCR understanding. Analyze the image carefully and generate five diverse text-centric questions, each paired with a concise answer. Questions should require reading and reasoning over visible text in the image, such as signs, labels, logos, or printed content. They may involve exact text extraction or simple reasoning based on the text.

All answers must be directly grounded in clearly visible text and be unambiguous. Avoid paraphrasing for the answers.

### Template Prompt for Identification Task

The primary goal of this task is to generate high-quality VQA questions for object identification. Analyze the image carefully and generate five diverse identification questions, each paired with a concise answer.

Questions should require recognizing and naming objects, entities, or scene elements present in the image based on their functional role, spatial position, or contextual relationships with other objects.

### Template Prompt for Comparison Task

The primary goal of this task is to generate high-quality VQA questions for comparison reasoning. Analyze the image carefully and generate five diverse comparison questions, each paired with a concise answer.

Questions should require comparing two or more objects, entities, or regions in the image based on attributes such as size, color, shape, quantity, position, or other visually observable properties. They may involve identifying differences, similarities, or determining which object satisfies a given condition

### Template Prompt for Spatial Task

The primary goal of this task is to generate high-quality VQA questions for spatial understanding. Analyze the image carefully and generate five diverse spatial reasoning questions, each paired with a concise answer. Questions should involve spatial relations such as left/right, above/below, in front of/behind, inside/outside, near/far, between, surrounding, or relative position.

### Template Prompt for Counting Task

The primary goal of this task is to generate high-quality VQA questions for counting task. Analyze the image carefully and generate five diverse counting reasoning questions (hard and very hard), each paired with an answer. The questions may involve basic counting, attribute-aware counting, or spatial counting. Label each question with a difficulty level.

Difficulty Guidelines: {}

### Template Prompt for Hallucination-Aware VQA

The primary goal of this task is to generate hallucination-based VQA questions that probe whether a model relies on non-existent or unsupported visual evidence. Analyze the image carefully and generate three hallucination questions.

Each question should be formulated such that it refers to objects, attributes, text, or relations that are not present in the image, or cannot be verified from the visual content, while remaining consistent with the specified task {task}. The goal is to test whether a model incorrectly assumes the presence of such elements.

Answers should be concise and reflect the absence of evidence.

## A.8 Prompt for LLM-as-a-Judge Evaluation of Answer Correctness

### Prompt

You are an evaluator for a visual question answering task. Your task is to determine whether the predicted answer is correct with respect to the ground-truth answer for the given question.

Evaluation rules:

1. Accept minor wording differences, paraphrases, singular/plural variation, and equivalent expressions.
2. Accept answers that are semantically equivalent to the ground-truth answer.
3. Reject answers that are incomplete, overly vague, or refer to the wrong object, attribute, count number, text, or relation.
4. For counting questions, the numeric value must match exactly unless the reference explicitly allows a range.
5. For OCR questions, ignore capitalization and minor punctuation differences, but do not ignore incorrect characters or different words.
6. For hallucination questions, accept only answers that clearly indicate the target does not exist or is not present or the answer cannot be determined from the image.
7. Be strict: the predicted answer should mean the same thing as the ground-truth answer in the context of the question.

Return your decision in JSON with the following fields:

```
{
  "correct": 0 or 1,
  "reason": "short explanation"
}
Question: {question}
Ground-truth answer: {gt-answer}
Predicted answer: {pred-answer}
Task type: {task-type}
Domain: {domain}
```

## A.9 Structured Output Format

Models are required to produce structured outputs consisting of a textual answer and corresponding multi-instance grounded visual evidence in a predefined format. For models that do not natively support structured grounding outputs, predicted regions are mapped to this format via post-processing. If no grounded object is present (*e.g.*, hallucination cases), the masks field is empty.

### Structured Output Template

```
{
  "image":
  {
    "image_id": {<id>},
    "width": H,
    "height": W,
    "file_name": "{<name>}"
  },
  "question": "<input question>",
  "prediction": {
    "text": "<final answer with optional object references>",
    "masks": [
      {"size": [H, W], "counts": "<RLE-encoded mask for instance1>"},
      {"size": [H, W], "counts": "<RLE-encoded mask for instance2>"}
      .
      .
      .
    ]
  }
}
```